crystals

MDPI

Article

Impurity-Induced Spin-State Crossover in $La_{0.8}Sr_{0.2}Co_{1-x}Al_xO_3$

Ichiro Terasaki *, Masamichi Ikuta, Takafumi D. Yamamoto and Hiroki Taniguchi

Department of Physics, Nagoya University, Nagoya 464-8602, Japan;
ikuta.masamichi@b.mbox.nagoya-u.ac.jp (M.I.); tdyamamoto@nagoya-u.jp (T.D.Y.);
hiroki_taniguchi@cc.nagoya-u.ac.jp (H.T.)
* Correspondence: terra@nagoya-u.jp; Tel./Fax: +81-52-789-5255

Received: 26 September 2018; Accepted: 29 October 2018; Published: 31 October 2018

Abstract: We have prepared a set of polycrystalline samples of $La_{0.8}Sr_{0.2}Co_{1-x}Al_xO_3$ ($0 \leq x \leq 0.2$), and have measured the magnetization as functions of temperature and magnetic field. We find that the average spin number per Co ion (S_{Co}) evaluated from the room-temperature susceptibility is around 1.2–1.3 and independent of x. However, we further find that S_{Co} evaluated from the saturation magnetization at 2 K is around 0.3–0.7, and decreases dramatically with x. This naturally indicates that a significant fraction of the Co^{3+} ions experience a spin-state crossover from the intermediate- to low-spin state with decreasing temperature in the Al-substituted samples. This spin-state crossover also explains the resistivity and the thermopower consistently. In particular, we find that the thermopower is anomalously enhanced by the Al substitution, which can be consistently explained in terms of an extended Heikes formula.

Keywords: cobalt oxide; spin polaron; impurity effect; spin-state crossover

1. Introduction

The spin state is one of the most fundamental concepts in transition-metal oxides/complexes [1]. The d electrons in a transition-metal ion feel the Coulomb repulsion from the neighboring oxygen anions. In a transition-metal ion surrounded with octahedrally-coordinated oxygen anions, the five-fold degenerate d orbitals in a vacuum are split into the triply degenerate t_{2g} orbitals and the doubly degenerate e_g orbitals. An energy gap from t_{2g} to e_g levels is called "ligand field splitting", and competes with the Hund coupling [2]. For a larger ligand field splitting, the d electrons occupy the t_{2g} levels first to minimize the total spin number S. On the other hand, for a larger Hund coupling, S is maximized to satisfy Hund's rule. The former state is called the low-spin state, and the latter the high-spin state.

While the two spin states can be seen from d^4 to d^7 electron systems, Co^{3+} is of particular importance in the sense that the low-spin state ($e_g^0 t_{2g}^6$, $S = 0$) and the high-spin state ($e_g^2 t_{2g}^4$, $S = 2$) are almost degenerate in energy, in which various external conditions such as temperature, pressure, and magnetic field can induce the spin-state transition/crossover [3]. $LaCoO_3$ [4–7] and $Sr_3YCo_4O_{10.5}$ [8–11] are prime examples.

In addition to the high- and low-spin states, the intermediate-spin state ($e_g^1 t_{2g}^5$, $S = 1$) has been theoretically proposed in the Co^{3+} oxides, [12] and has been controversial for long time. Nakao et al. [13] have observed the characteristic resonant X-ray diffraction in a single-crystal sample of $Sr_3YCo_4O_{10.5}$ at low temperatures, indicating an e_g-like elongated electron density distribution around the Co^{3+} ion. This naturally suggests that the Co^{3+} ions are in the intermediate-spin state. In the case of $LaCoO_3$, however, no critical experiments have been done thus far, and it is still under debate whether or not the intermediate-spin state exists [14–20]. Recently, the intermediate-spin state

has been regarded as a kind of excitonic insulator from the low-spin state, [21–23] and its excited properties have been reinvestigated [24].

In contrast to the undoped $LaCoO_3$, researchers in the community seem to reach a consensus that the Co^{3+} ions exist as the intermediate-spin state in the doped $LaCoO_3$, and are responsible for the ferromagnetic metal state (FMM) in the heavily-doped samples [25–29]. Figure 1 shows an electronic phase diagram of $La_{1-x}Sr_xCoO_3$ simplified from the original one [30]. Note that the FMM phase shows cluster glass behavior, however, we do not further explore the glass nature of this phase in this paper. For $x \ll 0.05$, the system is insulating, and the magnetic Co^{3+} ions experience the spin-state crossover denoted by the reverse triangles, showing the nonmagnetic ground state. According to this figure, the spin-state crossover is quickly suppressed with increasing Co^{4+} content x. This has been explained in terms of spin polaron, [31] which is a spin cluster consisting of one Co^{4+} ion in the low-spin state surrounded by several Co^{3+} ions in the intermediate-spin state [32].

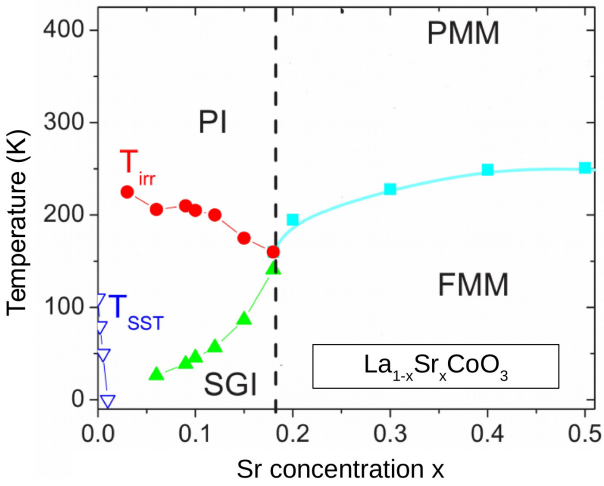

Figure 1. Phase diagram of $La_{1-x}Sr_xCoO_3$ simplified from the original one in Reference [30]. Depending on Sr content x and temperature, the system takes the paramagnetic insulator (PI), the spin glass insulator (SGI), the paramagnetic metal (PMM), or ferromagnetic metal (FMM) state. FMM is often indistinguishable from cluster glass state. The reverse triangles show the spin-state crossover temperature T_{SST}. The other marks correspond to magnetic transition temperatures.

In this paper, we report on the effects of Al substitution for Co on the magnetic and transport properties of doped $LaCoO_3$. Impurity has been a powerful test for the essential properties of novel materials. Bardeen-Cooper-Schrieffer-type superconductors are robust against nonmagnetic impurities which is demonstrated in the Anderson theorem, but are very susceptible against magnetic impurity as explained by the Abrikosov-Gor'kov theory [33]. For unconventional superconductors, nonmagnetic impurity has revealed various anomalous properties in the high-temperature superconducting copper oxides, [34] and possible orbital-fluctuation-driven superconductivity in the Fe-based superconductors [35]. How the impurity effects deviate from simple dilution effects and/or percolation theories in various magnetic materials has been discussed. The Haldane chain compound exhibits anomalous $S = 1/2$ excitation on the Ni^{2+} chain against Cu^{2+} impurity doping, [36] and a transition from the dimered to uniform antiferromagnetic order is observed in Mg-doped $CuGeO_3$ [37]. In the case of $LaCoO_3$, Kyomen et al. [38] conducted a pioneering study focused on this, and they have found that the Rh substitution enhances the paramagnetism, while the Al and Ga substitution increases the spin-state crossover temperature to stabilize the low-spin state. Following their work, we studied the Co-site substitution effects in the doped and undoped $LaCoO_3$. In particuar, Asai et al. [39] found a weak ferromagnetism in $LaCo_{1-x}Rh_xO_3$, below around 15 K for $0.1 \leq x \leq 0.4$, which can be regarded as a ferromagnetism emerging from nonmagnetic end phases. As a natural extension, we conducted an extensive study of the Al-substitution effect in the doped $LaCoO_3$, where the carrier concentration is

set to 0.2 per Co because metallic conduction is reported in this carrier concentration. Here we propose that spin-state crossover takes place in the doped $LaCoO_3$, and the substitution of Al for Co excellently highlights this crossover.

2. Experimental

Polycrystalline samples of $La_{0.8}Sr_{0.2}Co_{1-x}Al_xO_3$ (x = 0, 0.05, 0.10, and 0.15) were prepared by a standard solid-state reaction. Stoichiometric amounts of La_2O_3, $SrCO_3$, Co_3O_4, and Al_2O_3 powders were mixed and calcined at 1273 K for 24 h in air. The calcined powder was ground and pressed into pellets, and sintered at 1473 K for 48 h in air.

The X-ray diffraction pattern was taken with a laboratory X-ray diffractometer (RINT-2200, Rigaku) in θ-2θ scan mode with Cu Kα as an X-ray source. The temperature dependence of the magnetization was measured with an SQUID susceptometer (MPMS, Quantum Design) in a field-cooling process in 0.1 T from 4 to 300 K. The magnetization–field curve was measured with the SQUID susceptometer from −7 to 7 T. The resistivity was measured with a four-probe technique with a homemade measurement station from 4 to 300 K in a liquid He cryostat. The thermopower was measured with a steady state and two-probe technique from 4 to 300 K in a liquid He cryostat. The sample bridged two separated copper heat baths, and the resistance heater made temperature differences between the two heat baths, which was monitored through a copper-constantan differential thermocouple. The contribution of the voltage leads were carefully subtracted.

3. Results

Figure 2 shows X-ray diffraction patterns of the prepared samples measured at room temperature. All the peaks are indexed as rhombohedral ($R\bar{3}c$), and no impurity phases are seen. The lattice parameter a slightly decreased with increasing Al content x (a = 5.440, 5.434, 5.429, and 5.421 Å for x = 0, 0.05, 0.10, and 0.15, respectively), and this indicates that the Al ion substituted well for Co in the whole set of the samples.

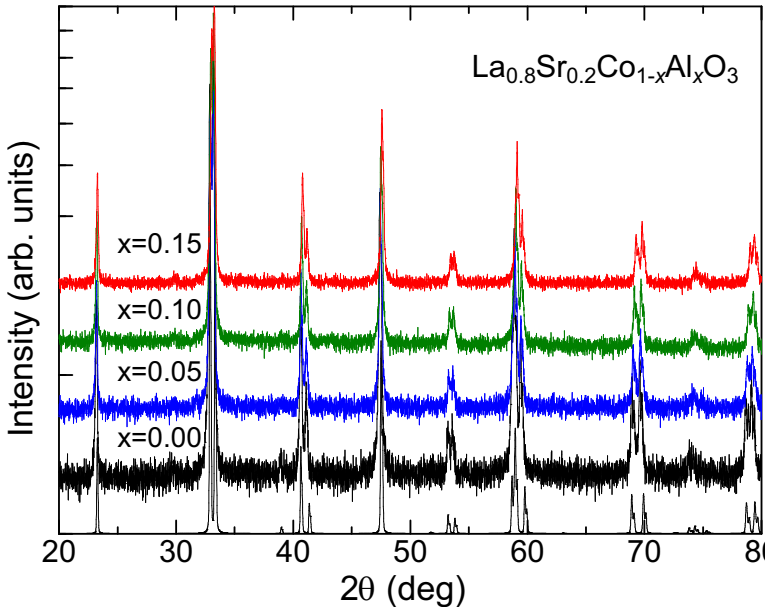

Figure 2. X-ray diffraction patterns of polycrystalline samples of $La_{0.8}Sr_{0.2}Co_{1-x}Al_xO_3$. The black curve plotted at the lowest position indicates the simulated diffraction patterns.

Figure 3a shows the temperature dependence of the magnetization in an external field of 0.1 T in the field-cooling process. All the samples showed a gradual increase in the magnetization below a certain temperature, indicating weak-ferromagnetic or cluster glass-like behavior. The data for $x = 0$ are consistent with preceding studies, [25–27] and the Al substitution systematically suppressed the

low temperature magnetization and the transition temperature. As the Al ion is chemically stable as trivalent, it substitutes for Co^{3+}. Thus, the present results suggest that Co^{3+} ions play a vital role in the FMM phase of the doped $LaCoO_3$, although FMM is driven by the doped holes (i.e., the Co^{4+} ions). For $x > 0$, a broad maximum is seen in the magnetization as indicated by the arrows. The physical meaning of this maximum will be discussed later.

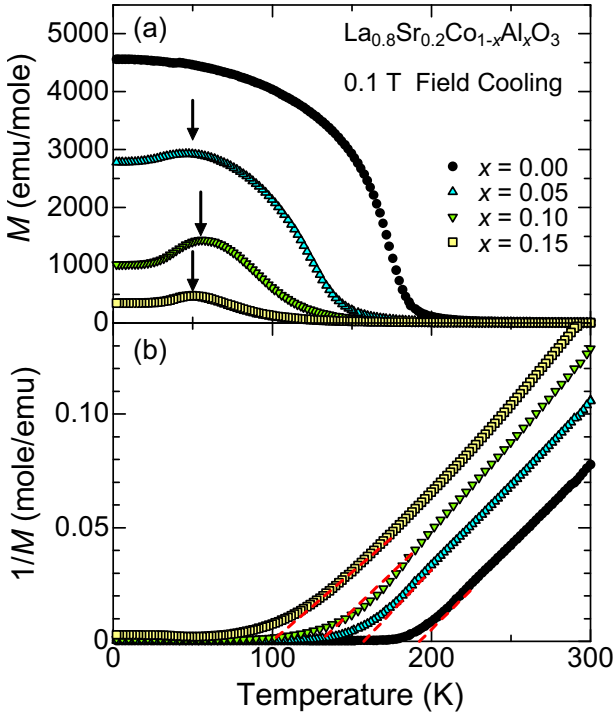

Figure 3. (**a**) Magnetization of polycrystalline samples of $La_{0.8}Sr_{0.2}Co_{1-x}Al_xO_3$ in an external field of 0.1 T in the field-cooling process. The arrows indicate a broad peak in the magnetization curve. (**b**) Inverse magnetization of the same data of (**a**). The black circles, blue triangles, green reverse triangles, and yellow squares represent x = 0, 0.05, 0.10 and 0.15, respectively. The dotted lines are guides to the eye for estimation of the transition temperature.

To see the transition temperature T_c and the susceptibility at high temperatures clearly, Figure 3b shows the inverse magnetization for the same data. Although the transition is broadened with increasing x, T_c decreases from 190 K for x = 0 down to 100 K for x = 0.15, as was estimated from the intersection points between the dotted lines and the temperature axis. This suppression is severer by a factor of three than the prediction from a simple dilution effect ($T_c(x)/T_c(0) \sim 1 - 3x$). This means that the Al substitution dramatically alters the ferromagnetic order. In contrast, the inverse magnetization above 250 K shows that the temperature slope is nearly the same for all the samples, and can be explained with a simple Curie–Weiss law in which the slope corresponds to the density of the magnetic moment. This indicates that the Al substitution left the whole number of magnetic moment almost unchanged. On one hand, this seems reasonable because Al^{3+} is nonmagnetic, but on the other hand it is in contradiction with the strong suppression of the ferromagnetic order.

Figure 4a shows the magnetization hysteresis plotted as a function of external field for all the samples at 2 K. We show only the positive magnetization part just for clarity. All the curves tend to saturate at high magnetic fields, which is a hallmark of ferromagnetism. The saturation magnetization is around 1.3 μ_B/f.u. for $x = 0$, while that for $x = 0.05$ it is around 1.0 μ_B/f.u. This indicates that 5% substituted Al decreases the saturation moment of 0.3 μ_B/f.u., i.e., one Al ion decreases a substantial value 6 μ_B. For further substitution, the decrease in saturation magnetization is somewhat tempered, but still one Al ion suppresses roughly 4 μ_B. Another notable feature is that the Al substitution makes the ferromagnetism harder; it increases the coercive field drastically. Owing to this hardening,

the magnetization in 0.1 T shown in Figure 3a was measured as being smaller values than expected which underestimate the saturation magnetization.

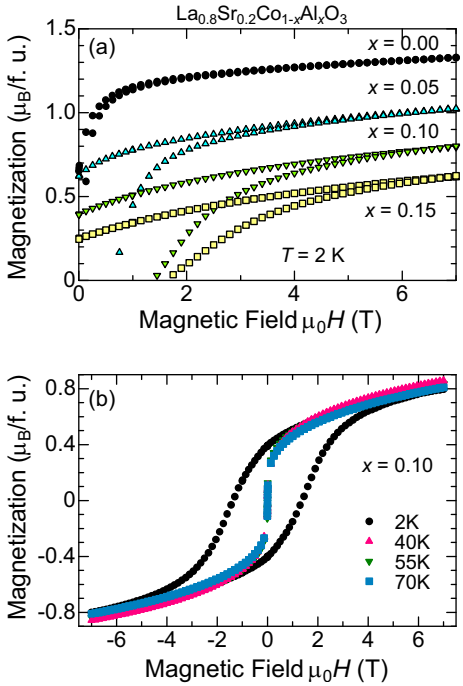

Figure 4. (**a**) Magnetization–field curve of polycrystalline samples of $La_{0.8}Sr_{0.2}Co_{1-x}Al_xO_3$ at 2 K. The positive magnetization part is shown for clarity. (**b**) The magnetization–field curves for x = 0.10 at various temperatures.

Figure 4b shows how the magnetic hysteresis evolves with temperature for $x = 0.10$. At 2 K, the magnetic hysteresis shows a clear loop with the coercive field of 1.5 T as was already mentioned above. With increasing temperature, the coercive field rapidly decreases above 40 K, and the magnetization does not show appreciable temperature dependence up to 70 K.

Let us evaluate the average spin number per Co ion quantitatively. We fit the magnetization above 250 K using the Curie–Weiss formula given by

$$\frac{M}{H} = \frac{C}{T - T_c}. \tag{1}$$

The parameter C is the Curie constant which is further written by

$$C = \frac{N\mu_{\text{eff}}^2}{3k_B} = \frac{Ng^2\mu_B^2 S(S+1)}{3k_B}, \tag{2}$$

where μ_{eff} is the effective magnetic moment, N the density of the effective moment, and S the effective spin number. Figure 5 shows the thus evaluated μ_{eff} plotted as a function of the Al content x. Clearly μ_{eff} is almost independent of x (slightly decreases with x), which is consistent with the fact that the temperature slope of the inverse magnetization is almost independent of x as was already discussed in Figure 3b. In contrast, the saturation magnetization below T_c rapidly decreases with x. We regard the magnetization at 7 T at 2 K ($M_{7\text{T}}$) as the saturation magnetization, and plot in the same figure.

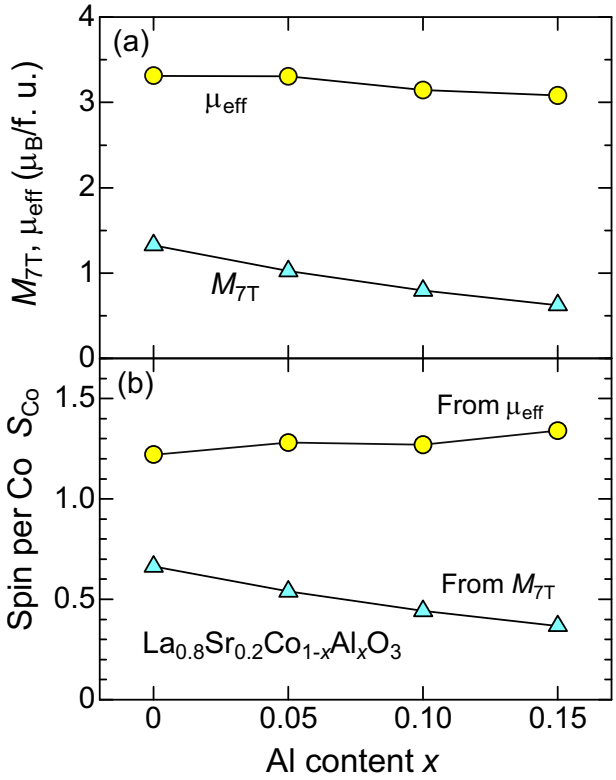

Figure 5. (**a**) Magnetization at 7 T (M_{7T}) evaluated from the magnetization–field curve at 2 K and the effective magnetic moment μ_{eff} evaluated from the Curie–Weiss fitting from 250 to 300 K. (**b**) The average spin number per Co (S_{Co}) evaluated from M_{7T} and μ_{eff}.

We evaluate the average spin number per Co (S_{Co}) from μ_{eff} and M_{7T}. In Figure 5b we plot the two kinds of S_{Co}, where we assume the g-factor to be 2. From μ_{eff}, S_{Co} is around 1.2–1.3 and almost independent of x. This suggests that most of the Co^{3+} ions are in the intermediate state (S = 1). On the other hand, from M_{7T}, S_{Co} is much smaller than unity and decreases with x. By combining these two, we are led to the conclusion that S_{Co} decreases with decreasing temperature, and such tendency becomes more remarkable upon the Al substitution. This naturally indicates that some portion of the Co ions show a crossover to the low-spin state at low temperatures.

We think that the spin-state crossover is the origin for the broad maximum observed in the magnetization for $x > 0$ in Figure 3a, which looks similar to the drop of the magnetization in $Sr_3YCo_4O_{10.5}$ around 200 K [8,40]. Since the two S_{Co} values do not coincide for x = 0, we propose that a small fraction of the Co^{3+} ions may experience spin-state crossover even for x = 0. This conclusion is consistent with the magnetic-resonance experiment by Smith et al. [41], from which they propose that the spin-state transition survives around 100 K up to 15% doped $LaCoO_3$. In $La_{1-x}Sr_xCoO_3$, Rodoriguez and Goodenough [26] have reported S_{Co} above T_c is almost independent of Sr content, while S_{Co} below T_c is much smaller and depends on Sr content. Kriener et al. [29] have found that the saturation magnetization is smaller in $La_{1-x}Ca_xCoO_3$ than in $La_{1-x}Sr_xCoO_3$ for the same x, which cannot be explained by a simple combination of the low-spin state Co^{4+} and the intermediate-spin state Co^{3+}. Prakash et al. [42] have also reported that the magnetization curves in $La_{1-x}Ca_xCoO_3$ are quantitatively different from those in $La_{1-x}Sr_xCoO_3$ in the form of nano-particles.

4. Discussion

4.1. Effects on Transport Properties

Let us discuss the effects of the Al substitution on the charge transport. Figure 6a shows the resistivity of the prepared samples plotted as a function of temperature. The resistivity for x

= 0 shows a low value of 1 mΩcm at room temperature, and weakly depends on temperatures above 100 K. With decreasing temperatures below 100 K, it turns into nonmetallic conduction, which has been regarded as the strong localization of carriers. This nonmetallic behavior happens when the double-exchange hopping between Co^{3+} and Co^{4+} ions is gradually suppressed below the magnetic transition temperature. The Al substitution increases the resistivity systematically at all temperatures, and makes the low-temperature upturn remarkable. We should note that the Al ions are expected to replace Co^{3+} ions in the system, thereby leaving the carrier concentration (the Co^{4+} concentration) intact. This is supported by the fact that the room-temperature resistivity remains in the order of mΩcm. Accordingly, we attribute the nonmetallic behavior to the reduced mobility arising from the localization of the spin polaron.

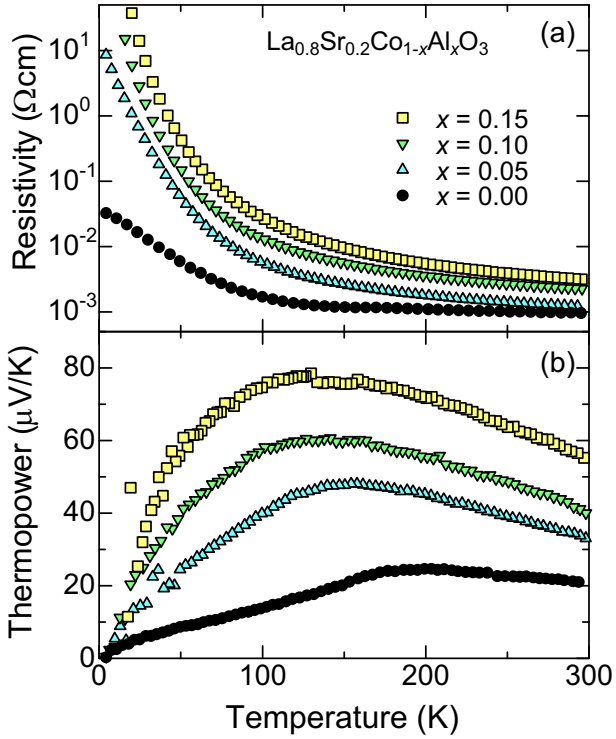

Figure 6. (**a**) Resistivity and (**b**) Thermopower of $La_{0.8}Sr_{0.2}Co_{1-x}Al_xO_3$.

Figure 6b shows the thermopower of the same set of the samples plotted as a function of temperature. The thermopower for x = 0 shows a small value of 20 μV/K at room temperature, and shows weak temperature dependence above the Curie temperature T_c of 190 K. Then it shows a broad kink at T_c, and shows a temperature-linear dependence which is expected in the thermopower of degenerate semiconductors [43]. Since the diffusion term does not include scattering time directly, the T-linear thermopower is not in contradiction to the nonmetallic resistivity upturn as a result of the localization.

Most notably, the Al substitution systematically enhances the thermopower at all the temperatures. The increment in the thermopower reaches 60 μV/K at 100 K from x = 0 to 0.15, which is quite substantial. The T-linear thermopower at low temperatures indicates that their electronic states are essentially metallic without an energy gap in the density of states, being consistent with the picture of localized spin polaron. The samples for x = 0.05, 0.10, and 0.15 show a broad peak, and the peak temperature decreases with x. The peak temperature seems to decrease with x similarly to T_c, but the relationship between the two temperatures is yet to be explored. We should note once again that the Al ions are supposed to replace Co^{3+} rather than Co^{4+}. Within a simple semiconductor physics, the thermopower depends mainly on the carrier concentration, not on the mobility. Thus, it is expected

to be related to the Co^{4+} concentration, but not to the Co^{3+} concentration. Thus, the thermopower enhancement induced by the Al substitution is highly nontrivial.

The thermopower of the cobalt oxides has been discussed in terms of an extended Heikes formula proposed by Koshibae et al. [44]. The theoretical expression is given by

$$S = \frac{k_B}{e} \ln \frac{g_A}{g_B} \frac{p}{1-p}, \quad (3)$$

where p is the concentration of the A ions, and g_i (i = A and B) is the internal electronic degeneracy due to the spin and orbital degrees of freedom. In the present case, p equals 0.2 (the Co^{4+} concentration) for all the samples. Consequently, $\ln g_{Co^{4+}}/g_{Co^{3+}}$ should determine the magnitude of the thermopower. We experimentally showed that the Co^{3+} ions in the low-spin state can give a large value of $\ln g_{Co^{4+}}/g_{Co^{3+}}$ [45–47].

In this respect, we can associate the thermopower enhancement at low temperatures with the spin-state crossover induced by Al substitution. Although the spin-state crossover is suggested at low temperatues from the magnetic measurements, the thermopower already increases at room temperature. We do not yet understand this clearly. One possibility is that the substituted Al ions bring additional entropy into the system, and give additional thermopower in the Heikes formula (g_A for Al ion and g_B for Co ion in Equation (3)). Another possibility is that the formation of the spin polaron gradually starts from room temperature, and is suppressed by the Al substitution. Consequently, the Co^{4+} ion is not fully surrounded with the intermediate-spin state Co^{3+} at room temperature.

4.2. Comparison with Other Impurities

In this subsection, we review the Co-site substitution effects on $LaCoO_3$ and the related cobalt oxides. After the pioneering work of Kyomen et al. [38], we have studied the Co-site substitution effects in the doped and undoped $LaCoO_3$. Asai et al. [39] found that the Rh substitution induces weak ferromagnetism in $LaCo_{1-x}Rh_xO_3$ and further found that the Ga substitution in the weak-ferromagnetic $LaCo_{0.8}Rh_{0.2}O_3$ severely suppresses the effective moment in the Co site [48]. These two works suggest that the Rh substitution stabilizes the Co^{3+} ion in the high-spin state, while the Ga substitution does the Co^{3+} ion in the low-spin state [49]. Knizek et al. [50] have reported from GGA+U electronic structure calculations that the Rh impurity can stabilize the high-spin state of the neighboring Co^{3+} ion. This tendency was further verified from optical reflectivity [51] and from X-ray absorption [52]. From the Curie–Weiss analysis, one substituted Rh ion leaves the value of S_{Co} unchanged up to 50% substitution, while one substituted Ga ion reduces S_{Co} by 4.6 μ_B. Tomiyasu et al. [53] have recently shown that the doped magnetic impurity, such as Cr^{3+}, Fe^{3+}, Mn^{4+}, or Ni^{2+}, is surrounded by magnetic Co ions in $LaCoO_3$.

In the case of the doped $LaCoO_3$, Shibasaki et al. [54] found that the Rh substitution in $La_{0.8}Sr_{0.2}Co_{1-x}Rh_xO_3$ does not change S_{Co} above T_c while one Rh substitution effectively decreases S_{Co} by 9 μ_B below T_c. Since their findings are qualitatively the same as those in the present work, we can also explain the big drop in S_{Co} from room temperature down to 5 K in $La_{0.8}Sr_{0.2}Co_{1-x}Rh_xO_3$ in terms of spin-state crossover. As mentioned in the previous section, one Al substitution decreases S_{Co} by 6 μ_B in $La_{0.8}Sr_{0.2}Co_{1-x}Al_xO_3$. It is not clear at present whether or not the difference between 9 μ_B for Rh and 6 μ_B for Al is intrinsic. One possibility is that the Rh ion destroy the spin polaron more seriously than the Al ion. While the 10% Rh substituted sample is nearly paramagnetic [54], the 10% Al substituted sample still shows ferromagnetic behavior.

4.3. An Origin of Impurity-Induced Spin-State Crossover

Let us discuss a possible mechanism of spin-state crossover induced by impurities. As already mentioned, the spin polaron is formed in the lightly-doped $LaCoO_3$. Podlesnyak et al. [31] have shown that the doped hole exists in the low-spin state Co^{4+} ion and is surrounded by six

octahedrally-coordinated Co^{3+} ions in the intermediate spin state. The intermediate-spin state Co^{3+} is believed to be induced by Co^{4+} in order that the doped hole can gain kinetic energy through the double exchange interaction. This spin polaron acts as a super-spin of $S = 13/2$ via the double exchange interaction within the cluster. From the earlier magnetic measurement, Yamaguchi et al. [32] have found that the magnetization–field curve can be fitted with a large spin number of $S = 10$–16, which is consistent with the spin-polaron picture. The above experiments consistently show that the unit of magnetic moment extends to several unit cells.

Thus, it is naturally expected that the doped Al replaces one of the Co^{3+} ions in the spin polaron, and suppresses the double exchange. In the strong coupling limit, a single Al ion can block the spin-polaron formation, and practically act as plural nonmagnetic ions. As already shown, the transition temperature is rapidly reduced with x roughly expressed by $T_c(x)/T_c(0) \sim 1 - 3x$. The factor of three may come from the picture that one Al ion effectively makes around three Co ions be in the low-spin state at low temperatures. This is consistent with the fact that one Al ion suppress 6 μ_B in the saturation magnetization.

Since S_{Co} is independent of x above T_c, the spin polaron is likely formed around T_c below which the effect of Al becomes remarkable. This is also suggested by the resistivity; the nonmetallic conduction becomes more remarkable below T_c. Since the spin polaron is strongly pinned or destroyed by the Al ion, it cannot act as a charge carrier in this system, where the isolated Co^{4+} ion is strongly localized in the sea of the low-spin state Co^{3+}. At room temperature where the spin polaron is not yet formed, the resistivity is weakly dependent on x.

4.4. Coercive Field Induced by Al Substitution

As was already mentioned in the previous section, the weak ferromagnetism becomes harder with increasing Al concentration as shown in Figure 4. The coercive field $\mu_0 H_c$ is unusually high, and reaches near 2 T at 2 K for $x = 0.15$. This is difficult to understand from a conventional theory of ferromagnets, [55] in which the anisotropy energy and the pinning force determine $\mu_0 H_c$. Accordingly, $\mu_0 H_c$ increases roughly with T_c in conventional hard ferromagnets. In the present case, however, $\mu_0 H_c$ *increases* and T_c *decreases* with x. In particular, the coercive energy of $\mu_0 H_c g \mu_B S_{Co}$ is of 2 K/f.u. for $x = 0.15$, which is comparable with the ferromagnetic energy of BH/f.u. at 6 T. In the first place, polycrystalline samples are expected to show smaller coercive field than single crystal [56].

Such giant coercive fields have been overlooked thus far, possibly because they are regarded as coming from extrinsic origins such as pinning centers, dislocations, and particle size [57]. Actually nano-size ferromagnetic particles of ε-Fe_2O_3 exhibit a giant coercive field of 2 T, [58] and three-atom-width nanowires of Co metal show $\mu_0 H_c = 1.2$ T [59].

Aside from nano-magnetics, huge coercive fields have been reported in various oxide materials. For example, $\mu_0 H_c$ equals 5.9 T at 4.2 K for $Co_2(OH)_2(C_8H_4O_4)$ [60], 9 T at 4.2 K for $LuFe_2O_4$ [61], 12 T at 2 K for the hexagonal $Sr_5Ru_{5-x}O_{15}$ [62], and 2 T at 100 K for $BaIrO_3$ [63]. Although the origin of these huge $\mu_0 H_c$ is different from material to material, a strong spin-orbit interaction and Ising-like anisotropy seem to play vital roles.

We have discussed a possible spin-state crossover induced by Al substitution. In this context, we can associate the giant $\mu_0 H_c$ with magnetic-field induced spin-state crossover. As was discussed above, the substituted Al ion pins the spin polaron, and lets the neighboring Co^{3+} ion be in the low-spin state. Since this pinning competes with the intra-polaron double exchange, we expect that the energy difference between the low- and intermediate-spin states is within the order of $k_B T$. In such a situation, an external field helps the intermediate-spin state to grow through the Zeeman effect, and the number of the intermediate spins gradually increases with increasing field. This is a kind of metamagnetic transition in the sense that the total spin number changes with external field, and accompanies a magnetic field hysteresis because the spin-state crossover causes a large magnetostriction [64]. The spin-state transition is induced by external field in $LaCoO_3$ and the related oxides, but the critical field is around 60 T for $LaCoO_3$ [65,66] and 53 T for $Sr_3YCo_4O_{10.5}$ [40]. It is not

surprising that they are much higher than those in the present case, because the spin-state crossover in the pure cobalt oxides is caused by a cooperative interaction among the Co^{3+} ions, while the spin-state energy and cooperative interaction are reduced near the Al impurity.

5. Summary

In summary, we prepared a set of polycrystalline samples of $La_{0.8}Sr_{0.2}Co_{1-x}Al_xO_3$ ($0 \leq x \leq 0.15$), and measured the X-ray diffraction, magnetization, resistivity, and thermopower. We obtained the average spin number per Co ion (S_{Co}) in two ways, and found that S_{Co} is around 1.2–1.3 at room temperature, and rapidly reduces to 0.3–0.7 at 2 K. The reduction of S_{Co} becomes more remarkable as x becomes larger. We have ascribed this to a spin-state crossover and proposed that the Al substitution enhances this crossover by pinning the spin polaron. The spin-state crossover also semi-quantitatively explains the enhanced thermopower and the anomalously large coercive field induced by the substituted Al ion.

Author Contributions: I.T. organized the while project, found the analysis method, and wrote the first draft of the manuscript. M.I. made and characterized the samples, and he measured and analyzed the magnetization with T.D.Y. All the authors equally contributed to the discussion and understanding of the experimental results.

Funding: This research received no external funding and the APC was funded by the operating expenses grants of Nagoya University.

Acknowledgments: The authors would like to thank K. Tanabe for collaboration, and for S. Asai, R. Okazaki and Y. Yasui for collaboration for the early study of the Co-site subsitution effects.

Conflicts of Interest: The authors declare no conflict of interest.

References

1. Gütlich, P.; Garcia, Y.; Goodwin, H.A. Spin crossover phenomena in Fe(II) complexes. *Chem. Soc. Rev.* **2000**, *29*, 419–427. [CrossRef]
2. Sugano, S.; Tanabe, Y.; Kamimura, H. *Multiplets of Transition-Metal Ions in Crystals*; Academic Press: New York, NY, USA, 1970.
3. Eder, R. Spin-state transition in $LaCoO_3$ by variational cluster approximation. *Phys. Rev. B* **2010**, *81*, 035101, doi:10.1103/PhysRevB.81.035101. [CrossRef]
4. Jonker, G.; Santen, J.V. Magnetic compounds wtth perovskite structure III. Ferromagnetic compounds of cobalt. *Physica* **1953**, *19*, 120–130. [CrossRef]
5. Raccah, P.M.; Goodenough, J.B. First-order localized-electron collective-electron transition in $LaCoO_3$. *Phys. Rev.* **1967**, *155*, 932–943. [CrossRef]
6. Asai, K.; Yoneda, A.; Yokokura, O.; Tranquada, J.M.; Shirane, G.; Kohn, K. Two spin-state transitions in $LaCoO_3$. *J. Phys. Soc. Jpn.* **1998**, *67*, 290–296. [CrossRef]
7. Vogt, T.; Hriljac, J.A.; Hyatt, N.C.; Woodward, P. Pressure-induced intermediate-to-low spin state transition in $LaCoO_3$. *Phys. Rev. B* **2003**, *67*, 140401. [CrossRef]
8. Kobayashi, W.; Ishiwata, S.; Terasaki, I.; Takano, M.; Grigoraviciute, I.; Yamauchi, H.; Karppinen, M. Room-temperature ferromagnetism in $Sr_{1-x}Y_xCoO_{3-\delta}$ ($0.2 \leq x \leq 0.25$). *Phys. Rev. B* **2005**, *72*, 104408. [CrossRef]
9. Kobayashi, W.; Yoshida, S.; Terasaki, I. High-temperature metallic state of room-temperature ferromagnet $Sr_{1-x}Y_xCoO_{3-\delta}$. *J. Phys. Soc. Jpn.* **2006**, *75*, 103702. [CrossRef]
10. Golosova, N.O.; Kozlenko, D.P.; Dubrovinsky, L.S.; Drozhzhin, O.A.; Istomin, S.Y.; Savenko, B.N. Spin state and magnetic transformations in $Sr_{0.7}Y_{0.3}CoO_{2.62}$ at high pressures. *Phys. Rev. B* **2009**, *79*, 104431. [CrossRef]
11. Sheptyakov, D.V.; Pomjakushin, V.Y.; Drozhzhin, O.A.; Istomin, S.Y.; Antipov, E.V.; Bobrikov, I.A.; Balagurov, A.M. Correlation of chemical coordination and magnetic ordering in $Sr_3YCo_4O_{10.5+\delta}$ (δ = 0.02 and 0.26). *Phys. Rev. B* **2009**, *80*, 024409. [CrossRef]
12. Korotin, M.A.; Ezhov, S.Y.; Solovyev, I.V.; Anisimov, V.I.; Khomskii, D.I.; Sawatzky, G.A. Intermediate-spin state and properties of $LaCoO_3$. *Phys. Rev. B* **1996**, *54*, 5309–5316. [CrossRef]

13. Nakao, H.; Murata, T.; Bizen, D.; Murakami, Y.; Ohoyama, K.; Yamada, K.; Ishiwata, S.; Kobayashi, W.; Terasaki, I. Orbital ordering of intermediate-spin state of Co^{3+} in $Sr_3YCo_4O_{10.5}$. *J. Phys. Soc. Jpn.* **2011**, *80*, 023711. [CrossRef]
14. Tokura, Y.; Okimoto, Y.; Yamaguchi, S.; Taniguchi, H.; Kimura, T.; Takagi, H. Thermally induced insulator-metal transition in $LaCoO_3$: A view based on the Mott transition. *Phys. Rev. B* **1998**, *58*, R1699–R1702. [CrossRef]
15. Noguchi, S.; Kawamata, S.; Okuda, K.; Nojiri, H.; Motokawa, M. Evidence for the excited triplet of Co^{3+} in $LaCoO_3$. *Phys. Rev. B* **2002**, *66*, 094404. [CrossRef]
16. Maris, G.; Ren, Y.; Volotchaev, V.; Zobel, C.; Lorenz, T.; Palstra, T.T.M. Evidence for orbital ordering in $LaCoO_3$. *Phys. Rev. B* **2003**, *67*, 224423. [CrossRef]
17. Haverkort, M.W.; Hu, Z.; Cezar, J.C.; Burnus, T.; Hartmann, H.; Reuther, M.; Zobel, C.; Lorenz, T.; Tanaka, A.; Brookes, N.B.; et al. Spin state transition in $LaCoO_3$ studied using soft X-ray absorption spectroscopy and magnetic circular dichroism. *Phys. Rev. Lett.* **2006**, *97*, 176405. [CrossRef] [PubMed]
18. Klie, R.F.; Zheng, J.C.; Zhu, Y.; Varela, M.; Wu, J.; Leighton, C. Direct measurement of the low-temperature spin-state transition in $LaCoO_3$. *Phys. Rev. Lett.* **2007**, *99*, 047203. [CrossRef] [PubMed]
19. Chakrabarti, B.; Birol, T.; Haule, K. Role of entropy and structural parameters in the spin-state transition of $LaCoO_3$. *Phys. Rev. Mater.* **2017**, *1*, 064403. [CrossRef]
20. Shimizu, Y.; Takahashi, T.; Yamada, S.; Shimokata, A.; Jin-no, T.; Itoh, M. Symmetry preservation and critical fluctuations in a pseudospin crossover perovskite $LaCoO_3$. *Phys. Rev. Lett.* **2017**, *119*, 267203. [CrossRef] [PubMed]
21. Nasu, J.; Watanabe, T.; Naka, M.; Ishihara, S. Phase diagram and collective excitations in an excitonic insulator from an orbital physics viewpoint. *Phys. Rev. B* **2016**, *93*, 205136. [CrossRef]
22. Sotnikov, A.; Kuneš, J. Field-induced exciton condensation in $LaCoO_3$. *Sci. Rep.* **2016**, *6*, 30510. [CrossRef] [PubMed]
23. Afonso, J.F.; Kuneš, J. Excitonic magnetism in d^6 perovskites. *Phys. Rev. B* **2017**, *95*, 115131. [CrossRef]
24. Wang, R.P.; Hariki, A.; Sotnikov, A.; Frati, F.; Okamoto, J.; Huang, H.Y.; Singh, A.; Huang, D.J.; Tomiyasu, K.; Du, C.H.; et al. Excitonic dispersion of the intermediate spin state in $LaCoO_3$ revealed by resonant inelastic X-ray scattering. *Phys. Rev. B* **2018**, *98*, 035149. [CrossRef]
25. Itoh, M.; Natori, I.; Kubota, S.; Motoya, K. Spin-glass behavior and magnetic phase diagram of $La_{1-x}Sr_xCoO_3$ $(0 \leq x \leq 0.5)$ studied by magnetization measurements. *J. Phys. Soc. Jpn.* **1994**, *63*, 1486–1493. [CrossRef]
26. Senarís-Rodríguez, M.A.; Goodenough, J.B. Magnetic and transport properties of the system $La_{1-x}Sr_xCoO_{3-\delta}$ $(0 < x \leq 0.50)$. *J. Solid State Chem.* **1995**, *118*, 323–336. [CrossRef]
27. Masuda, H.; Fujita, T.; Miyashita, T.; Soda, M.; Yasui, Y.; Kobayashi, Y.; Sato, M. Transport and magnetic properties of $R_{1-x}A_xCoO_3$ (R = La, Pr and Nd; A = Ba, Sr and Ca). *J. Phys. Soc. Jpn.* **2003**, *72*, 873–878. [CrossRef]
28. Wu, J.; Leighton, C. Glassy ferromagnetism and magnetic phase separation in $La_{1-x}Sr_xCoO_3$. *Phys. Rev. B* **2003**, *67*, 174408. [CrossRef]
29. Kriener, M.; Zobel, C.; Reichl, A.; Baier, J.; Cwik, M.; Berggold, K.; Kierspel, H.; Zabara, O.; Freimuth, A.; Lorenz, T. Structure, magnetization, and resistivity of $La_{1-x}M_xCoO_3$ (M = Ca, Sr, and Ba). *Phys. Rev. B* **2004**, *69*, 094417. [CrossRef]
30. He, C.; Torija, M.A.; Wu, J.; Lynn, J.W.; Zheng, H.; Mitchell, J.F.; Leighton, C. Non-Griffiths-like clustered phase above the Curie temperature of the doped perovskite cobaltite $La_{1-x}Sr_xCoO_3$. *Phys. Rev. B* **2007**, *76*, 014401. [CrossRef]
31. Podlesnyak, A.; Russina, M.; Furrer, A.; Alfonsov, A.; Vavilova, E.; Kataev, V.; Büchner, B.; Strässle, T.; Pomjakushina, E.; Conder, K.; et al. Spin-state polarons in lightly-hole-doped $LaCoO_3$. *Phys. Rev. Lett.* **2008**, *101*, 247603. [CrossRef] [PubMed]
32. Yamaguchi, S.; Okimoto, Y.; Taniguchi, H.; Tokura, Y. Spin-state transition and high-spin polarons in $LaCoO_3$. *Phys. Rev. B* **1996**, *53*, R2926–R2929. [CrossRef]
33. Gor'kov, L.P., Theory of superconducitng alloys. In *The Physics of Superconductors*; Chapter 5; Springer: Berlin, Germany, 2003. [CrossRef]
34. Fukuzumi, Y.; Mizuhashi, K.; Takenaka, K.; Uchida, S. Universal superconductor-insulator transition and T_c depression in Zn-substituted high-T_c cuprates in the underdoped regime. *Phys. Rev. Lett.* **1996**, *76*, 684. [CrossRef] [PubMed]

35. Kontani, H.; Onari, S. Orbital-fluctuation-mediated superconductivity in iron pnictides: Analysis of the five-orbital Hubbard-Holstein model. *Phys. Rev. Lett.* **2010**, *104*, 157001. [CrossRef] [PubMed]
36. Hagiwara, M.; Katsumata, K.; Affleck, I.; Halperin, B.I.; Renard, J. Observation of S = 1/2 degrees of freedom in an S = 1 linear-chain Heisenberg antiferromagnet. *Phys. Rev. Lett.* **1990**, *65*, 3181. [CrossRef] [PubMed]
37. Masuda, T.; Fujioka, A.; Uchiyama, Y.; Tsukada, I.; Uchinokura, K. Phase transition between dimerized-antiferromagnetic and uniform-antiferromagnetic phases in the impurity-doped spin-Peierls cuprate $CuGeO_3$. *Phys. Rev. Lett.* **1998**, *80*, 4566. [CrossRef]
38. Kyômen, T.; Asaka, Y.; Itoh, M. Negative cooperative effect on the spin-state excitation in $LaCoO_3$. *Phys. Rev. B* **2003**, *67*, 144424. [CrossRef]
39. Asai, S.; Furuta, N.; Yasui, Y.; Terasaki, I. Weak Ferromagnetism in $LaCo_{1-x}Rh_xO_3$: Anomalous magnetism emerging between two nonmagnetic end phases. *J. Phys. Soc. Jpn.* **2011**, *80*, 104705. [CrossRef]
40. Kimura, S.; Maeda, Y.; Kashiwagi, T.; Yamaguchi, H.; Hagiwara, M.; Yoshida, S.; Terasaki, I.; Kindo, K. Field-induced spin-state transition in the perovskite cobalt oxide $Sr_{1-x}Y_xCoO_{3-\delta}$. *Phys. Rev. B* **2008**, *78*, 180403. [CrossRef]
41. Smith, R.X.; Hoch, M.J.R.; Moulton, W.G.; Kuhns, P.L.; Reyes, A.P.; Boebinger, G.S.; Zheng, H.; Mitchell, J.F. Evolution of the spin-state transition with doping in $La_{1-x}Sr_xCoO_3$. *Phys. Rev. B* **2012**, *86*, 054428. [CrossRef]
42. Prakash, R.; Shukla, R.; Nehla, P.; Dhaka, A.; Dhaka, R. Tuning ferromagnetism and spin state in $La_{1-x}A_xCoO_3$ (A = Sr, Ca) nanoparticles. *J. Alloys Comp.* **2018**, *764*, 379–386. [CrossRef]
43. Terasaki, I. Thermal conductivity and thermoelectric power of semiconductors. In *Reference Module in Materials Science and Materials Engineering*; Elsevier: Amsterdam, The Netherlands, 2016. [CrossRef][CrossRef]
44. Koshibae, W.; Tsutsui, K.; Maekawa, S. Thermopower in cobalt oxides. *Phys. Rev. B* **2000**, *62*, 6869–6872. [CrossRef]
45. Terasaki, I.; Sasago, Y.; Uchinokura, K. Large thermoelectric power in $NaCo_2O_4$ single crystals. *Phys. Rev. B* **1997**, *56*, R12685–R12687. [CrossRef]
46. Yoshida, S.; Kobayashi, W.; Nakano, T.; Terasaki, I.; Matsubayashi, K.; Uwatoko, Y.; Grigoraviciute, I.; Karppinen, M.; Yamauchi, H. Chemical and physical pressure effects on the magnetic and transport properties of the A-site ordered perovskite $Sr_3YCo_4O_{10.5}$. *J. Phys. Soc. Jpn.* **2009**, *78*, 094711. [CrossRef]
47. Terasaki, I.; Shibasaki, S.; Yoshida, S.; Kobayashi, W. Spin State Control of the Perovskite Rh/Co Oxides. *Materials* **2010**, *3*, 786–799. [CrossRef]
48. Asai, S.; Furuta, N.; Okazaki, R.; Yasui, Y.; Terasaki, I. Ga^{3+} substitution effects in the weak ferromagnetic oxide $LaCo_{0.8}Rh_{0.2}O_3$. *Phys. Rev. B* **2012**, *86*, 014421. [CrossRef]
49. Asai, S.; Okazaki, R.; Terasaki, I.; Yasui, Y.; Kobayashi, W.; Nakao, A.; Kobayashi, K.; Kumai, R.; Nakao, H.; Murakami, Y.; et al. Spin State of Co^{3+} in $LaCo_{1-x}Rh_xO_3$ Investigated by Structural Phenomena. *J. Phys. Soc. Jpn.* **2013**, *82*, 114606. [CrossRef]
50. Knizek, K.; Hejtmánek, J.; Marysko, M.; Jirák, Z.; Bursik, J. Stabilization of the high-spin state of Co^{3+} in $LaCo_{1-x}Rh_xO_3$. *Phys. Rev. B* **2012**, *85*, 134401. [CrossRef]
51. Terasaki, I.; Asai, S.; Taniguchi, H.; Okazaki, R.; Yasui, Y.; Ikemoto, Y.; Moriwaki, T. Optical evidence for the spin-state disorder in $LaCo_{1-x}Rh_xO_3$. *J. Phys. Condens. Mat.* **2017**, *29*, 235802. [CrossRef] [PubMed]
52. Sudayama, T.; Nakao, H.; Yamasaki, Y.; Murakami, Y.; Asai, S.; Okazaki, R.; Yasui, Y.; Terasaki, I. Spin state of Co^{3+} in $LaCo_{1-x}Rh_xO_3$ studied using X-ray absorption spectroscopy. *J. Phys. Soc. Jpn.* **2017**, *86*, 094701. [CrossRef]
53. Tomiyasu, K.; Kubota, Y.; Shimomura, S.; Onodera, M.; Koyama, S.I.; Nojima, T.; Ishihara, S.; Nakao, H.; Murakami, Y. Spin-state responses to light impurity substitution in low-spin perovskite $LaCoO_3$. *Phys. Rev. B* **2013**, *87*, 224409. [CrossRef]
54. Shibasaki, S.; Terasaki, I.; Nishibori, E.; Sawa, H.; Lybeck, J.; Yamauchi, H.; Karppinen, M. Magnetic and transport properties of the spin-state disordered oxide $La_{0.8}Sr_{0.2}Co_{1-x}Rh_xO_{3-\delta}$. *Phys. Rev. B* **2011**, *83*, 094405. [CrossRef]
55. Kittel, C. Physical theory of ferromagnetic domains. *Rev. Mod. Phys.* **1949**, *21*, 541. [CrossRef]
56. Kronmüller, H. Theory of the coercive field in amorphous ferromagnetic alloys. *J. Mag. Mag. Mater.* **1981**, *24*, 159–167. [CrossRef]
57. Kneller, E.F.; Luborsky, F.E. Particle size dependence of coercivity and remanence of single-domain particles. *J. Appl. Phys.* **1963**, *34*, 656–658. [CrossRef]

58. Jin, J.; Ohkoshi, S.i.; Hashimoto, K. Giant coercive field of nanometer-sized iron oxide. *Adv. Mater.* **2004**, *16*, 48–51. [CrossRef]
59. Gambardella, P.; Dallmeyer, A.; Maiti, K.; Malagoli, M.C.; Rusponi, S.; Ohresser, P.; Eberhardt, W.; Carbone, C.; Kern, K. Oscillatory magnetic anisotropy in one-dimensional atomic wires. *Phys. Rev. Lett.* **2004**, *93*, 077203. [CrossRef] [PubMed]
60. Huang, Z.L.; Drillon, M.; Masciocchi, N.; Sironi, A.; Zhao, J.T.; Rabu, P.; Panissod, P. Ab-initio XRPD crystal structure and giant hysteretic effect (H c= 5.9 T) of a new hybrid terephthalate-based cobalt (II) magnet. *Chem. Mater.* **2000**, *12*, 2805–2812. [CrossRef]
61. Wu, W.; Kiryukhin, V.; Noh, H.J.; Ko, K.T.; Park, J.H.; Ratcliff, W.; Sharma, P.A.; Harrison, N.; Choi, Y.J.; Horibe, Y.; et al. Formation of pancakelike ising domains and giant magnetic coercivity in ferrimagnetic $LuFe_2O_4$. *Phys. Rev. Lett.* **2008**, *101*, 137203. [CrossRef] [PubMed]
62. Yamamoto, A.; Hashizume, D.; Katori, H.A.; Sasaki, T.; Ohmichi, E.; Nishizaki, T.; Kobayashi, N.; Takagi, H. Ten layered hexagonal perovskite $Sr_5Ru_{5-x}O_{15}$ (x = 0.90), a weak ferromagnet with a giant coercive field $H_c \sim 12$ T. *Chem. Mater.* **2010**, *22*, 5712–5717. [CrossRef]
63. Kida, T.; Senda, A.; Yoshii, S.; Hagiwara, M.; Nakano, T.; Terasaki, I. Pressure effect on magnetic properties of a weak ferromagnet $BaIrO_3$. *J. Phys. Conf. Ser.* **2010**, *200*, 012084. [CrossRef]
64. Sato, K.; Bartashevich, M.I.; Goto, T.; Kobayashi, Y.; Suzuki, M.; Asai, K.; Matsuo, A.; Kindo, K. High-field magnetostriction of the spin-state transition compound $LaCoO_3$. *J. Phys. Soc. Jpn.* **2008**, *77*, 024601. [CrossRef]
65. Sato, K.; Matsuo, A.; Kindo, K.; Kobayashi, Y.; Asai, K. Field induced spin-state transition in $LaCoO_3$. *J. Phys. Soc. Jpn.* **2009**, *78*, 093702. [CrossRef]
66. Altarawneh, M.M.; Chern, G.W.; Harrison, N.; Batista, C.D.; Uchida, A.; Jaime, M.; Rickel, D.G.; Crooker, S.A.; Mielke, C.H.; Betts, J.B.; et al. Cascade of magnetic field induced spin transitions in $LaCoO_3$. *Phys. Rev. Lett.* **2012**, *109*, 037201. [CrossRef] [PubMed]